Hydroelastic analysis of a fishing net in steady inflow conditions

Arne Fredheim
Department of Aquaculture Technology, SINTEF Fisheries and Aquaculture, Trondheim, Norway

Odd M. Faltinsen
Department of Marine Technology, Norwegian University of Science and Technology, Trondheim, Norway

ABSTRACT: A three-dimensional numerical model of the fluid flow, which takes into consideration the influence of the net structure on the flow, has been developed. To be able to model fluid-structure interaction, structural analysis using a FEM method is included. The net is divided into a set of cylindrical and spherical elements to represent the twines and knots of the net. The influence from the net structure on the fluid flow is then calculated by representing the wake generated by each element as source distributions along the structural element. The interaction between the net elements, due to the physical generation of a wake flow behind each individual element of the net, is based on a time-averaged wake model, applicable for the near-field wake. An examination of experimental results for the drag force on a plane net structure, show a strong dependency of both the geometry, in terms of Solidity ratio, and Reynolds number. This dependency is partly explained by the change in the drag coefficient for the individual elements which make up a net structure. For increasing Solidity ratios, the effect of the interaction between the different elements of the net on the drag force increases and has to be accounted for. Results for plane nets are presented and the influence of the knot part of the net on the drag force is discussed. Also results for a three-dimensional conical net structure are presented as drag forces and fluid velocity in front and inside of the net structure. Unfortunately there are not much published results related to analysis of three-dimensional net structures, but the results are sought validated against experimental results by Gustafson (1980) for drag on net structures and Enerhaug and Gjøsund (2001 and 2003) for the fluid velocity in front and inside of a conical net structure. The significance of the geometrical elasticity for the results is discussed.

1 INTRODUCTION

The resources of wild fish are limited. The trend in recent years has been that the amount of wild catch is stagnating. In this perspective the selectivity of fishing gear has become an important issue. The research so far has mainly focused on the testing of different sorting devices. Fig. 1 illustrates a trawl with a sorting device mounted in the aft part. In addition, numerical models have been developed to study the shape and behavior of both trawls and purse seines. All of these numerical models known to the authors are based on the assumption of undisturbed flow, both in front and inside the net structure. A three-dimensional net structure is however a highly flexible structure and the force acting on the structure due to the fluid flow will have an effect on the shape of the structure, and further will alter the influence of the net structure on the fluid flow. The aim of the present work is to develop a three-dimensional model for the flow in front and inside a net structure, such as a trawl. The flow conditions behind the trawl is not considered.

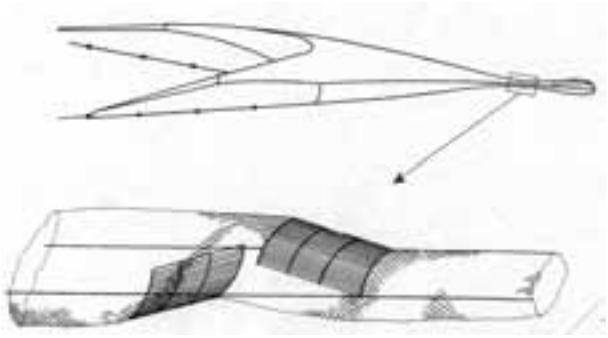

Fig. 1: Illustration of a trawl with a sorting device.

The motivation for this work is three folded. The most obvious is to improve the input flow model for a structural analysis of a net structure to account for the effect of the trawl on the inflow conditions. Secondly the possibility to study the flow conditions by it self. This to be able to analyze the velocity field within the trawl due to the shape of the trawl, the solidity of

the netting for the different parts of the trawl and the influence of any possible sorting devices. And finally the ability to study the pressure in front of the trawl, based on the assumption that the fish is able to detect the trawl due to an alternation of the experienced pressure field. However on what level the fish is able to detect small variations in the pressure field is unclear. It is more likely that the fish actually detect the trawl by visual means. The overall objective is to be able to improve the selectivity of the trawl.

2 MODELING

Using a structural finite element method combined with Navier-Stokes equations is impossible due to the required CPU time and data storage. Further CFD methods for this types of flow have clear physical limitations. Our objective is to develop simplified and physically justified methods. A structural analysis of the net structure using a FEM method has been included in the model. By combining the change in the inflow due to the presence of the net structure, which is a function of the shape and geometry of the net, with a correction of the shape and geometry due to the drag load, we get a more complete description of the problem. Further it is impractical to model every single twine in a net or a trawl. Typically the total number of twines could be in the order of 10^6.

Fig. 2 illustrate two different types of net panels, with square mesh and diamond mesh. The twines connect in knots and make up a mesh. The diameter of a twine can be from $1\,[mm]$ in net pens up to a few centimeters in the front part of a trawl. And similar the size of the mesh can be from $1\,[cm]$ up to the order of a meter. Typical Reynolds number range, related to the diameter of a twine, is $O(10^2 - 10^4)$. In net pens, used for aquaculture purposes, the square mesh type is mainly used, while in trawling normally the diamond mesh type is used. In open sea fish farming a constant flow of clean water is important, thus a square mesh orientation of the net, with constant and controlled mesh opening, is favored. In trawling other aspects are important, such as the distribution of tension within the net structure and actually that when exposed to drag force, the opening of the meshes in the aft part of a trawl will become smaller, and even closed. This also implies that there is less control of the actual opening of mesh while trawling, which is important with regards to selectivity. Thus the geometrical flexibility of the two mesh types is very different. This can be qualitatively understood by just pulling on each side of a net with different types of mesh. This also makes it inaccurate to compare results from a numerical analysis with square mesh, with experiments for a diamond mesh structure and vice versa.

The three-dimensional net structure is divided into discrete elements, by modeling the twines as separate

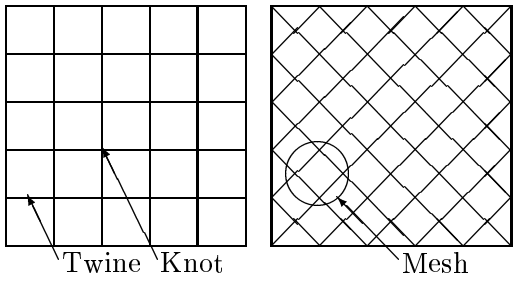

Fig. 2: Illustration of square mesh (top) and diamond mesh nets(bottom)

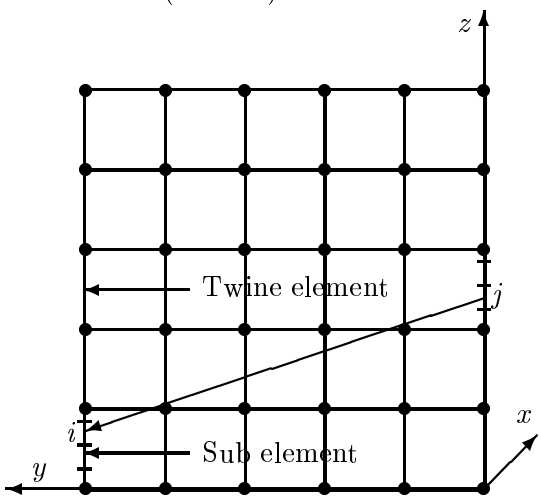

Fig. 3: Illustration of modeling of the net

cylinders between knots, with two-dimensional properties, allowing the interaction between them to be three-dimensional and the knots as separate spheres, with full three-dimensional properties. The modeling is illustrated in Fig. 3. Each of the twine elements between knots can further, but do not have to, be divided into sub elements, as illustrated in the figure. In the following, we do not distinguish between twine elements and sub elements, if not specifically stated that we are discussing sub elements. The total drag on the net will then become a sum of the drag of each of the individual elements. The drag on each element is calculated as the drag on a single circular cylinder in a two-dimensional free flow, which can be expressed as $\mathbf{F_c} = 1/2\rho C_D dL|\mathbf{U}|\mathbf{U}$, where $\mathbf{U}$ is the inflow velocity vector in a plane orthogonal to the cylinder axis. $|\mathbf{U}|$ is the magnitude of the inflow velocity, C_d is the drag coefficient for the cylinder, d is the diameter and L is the length of the cylinder. The expression for the drag on a sphere in three-dimensional free flow will in a similar fashion become $\mathbf{F_s} = \pi d^2/8\rho C_d|\mathbf{U}_{3D}|\mathbf{U}_{3D}$, where $\pi d^2/4$ is the projected area of the sphere.

First the influence from the net on the fluid flow is calculated by representing the wake generated by each element as source distributions along the structural element. To determine the strength of these sources the principle of Lagally is applied, which basically states

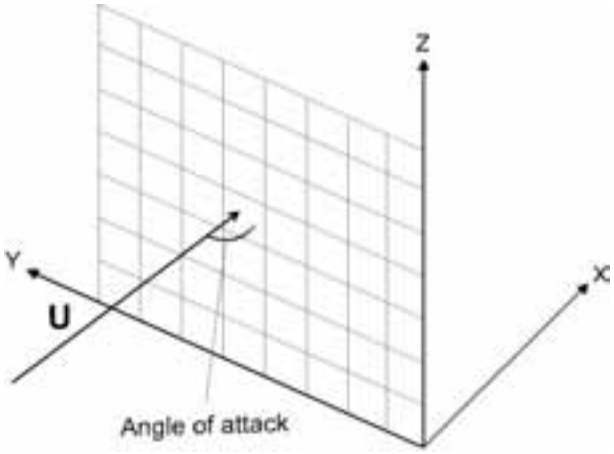

Fig. 4: Definition of angle of attack, α for plane net structures. It is assumed that the ambient inflow vector is restricted to be in the xy-plane.

that the force acting on a source of strength q in uniform flow is equal to the source strength times the incoming velocity times the fluid density. Thus a set of equations is obtained, describing the relation between the fluid velocity and the source strength at every element. And this leads to a model that describes the disturbance of the fluid flow in front of the net, due to the presence of the net. This is described more thoroughly in Fredheim and Faltinsen (2001).

Secondly the interaction between the net elements, due to the physical generation of a wake flow behind each individual element of the net, has been studied using a time-averaged velocity deficit model. Different models have been tried out. The basis for all the models, is the far field mean velocity deficit model for the flow behind a single cylinder described by Schlichting (1968). Modifications are applied, to better describe the near field behavior and the added effect on the total flow field due to the generation of the wake from the many individual cylindrical elements which make up the net. The reduced inflow for one element of the net due to the generated velocity deficit from all the proceeding elements are calculated. This makes it possible to analyze the current forces on a net structure at different angles of attack (see Fig. 4). More details in Fredheim and Faltinsen (2002).

Combining these two effects, together with a structural analysis, we get a complete model appropriate for analysis of current forces and response on three-dimensional net structures.

3 RESULTS AND DISCUSSION

3.1 *Analysis of a net structure*

There are four main parameters which are relevant when discussing the flow and drag force related to a net structure:

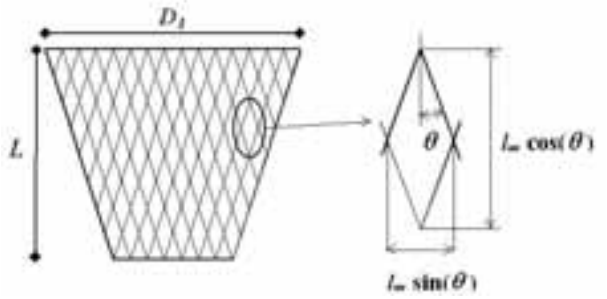

Fig. 5: Definition of mesh properties.

- the angle of attack, α for the net panel (see Fig. 4)
- the Solidity ratio, Sn, of the net,
- the Hanging ratios, E_1 and E_2, of the mesh and
- the Reynolds number, Rn, of the individual twines.

The Hanging ratio describes the diamond shape of the mesh and is a function of the angle of the mesh opening. Definitions are given in Fig. 5. In the crosswise direction of a net panel the hanging ratio is defined as:

$$E_1 = \frac{D_1 \pi}{T_1 l_m} = \sin\phi \tag{1}$$

and in the longitudinal direction as

$$E_2 = \frac{L}{N T_1 l_m} = \cos\phi \tag{2}$$

where D_1 is the diameter and T_1 is the number of meshes at the front part of the net panel, L is the length between the front and aft part of the net panel, N is the number of meshes in the longitudinal direction, l_m is the mesh opening and 2ϕ is the angle of the mesh opening.

The solidity ratio, Sn, describes the ratio of the projected area of the net, A_p, over the total area, A, enclosed by the net. In general the Solidity ratio will become a function of the Hanging ratios:

$$Sn = \frac{2d}{l_m E_1 E_2} - \left(\frac{d}{l_m}\right)^2 \left(\frac{1}{E_1^2} + \frac{1}{E_2^2}\right) \tag{3}$$

where d is the twine diameter. For a square mesh the angle of the mesh opening 2ϕ will become equal to 90°, and the Solidity ratio can be expressed as:

$$Sn = \frac{2d}{\lambda} - \left(\frac{d}{\lambda}\right)^2 \tag{4}$$

where λ is defined as the half mesh equal to $0.5\, l_m$ and is the same as the length of one side in a square mesh. I.e. Sn is a ratio related to the size relation between the diameter and mesh opening of a net.

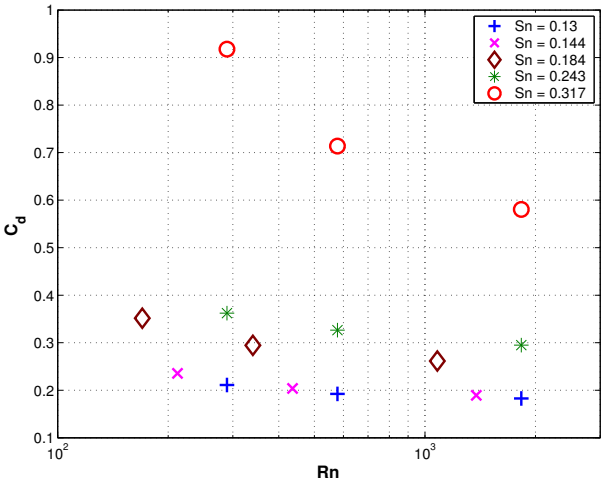

Fig. 6: Drag coefficient for plane nets with different solidity ratios at 90° angle of attack, as a function of Reynolds number. (Rudi *et al.*, 1988)

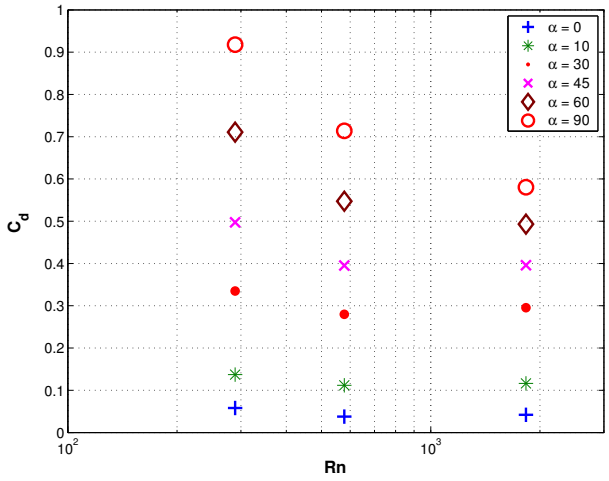

Fig. 7: Drag coefficient for a plane net with a Solidity ratio of 0.317 at different angles of attack, as a function of Reynolds number. (Rudi *et al.*, 1988)

The Reynolds number, which is an important parameter related to the flow around each twine and knot, is defined as:

$$Rn = \frac{U\,d}{\nu} \tag{5}$$

where ν is the kinematic viscosity and U is the incoming flow velocity. In addition while studying the detail flow around single twines, the Strouhal number, St, could play an important role.

In Fig. 6 and 7 results for the drag force on net panels as a function of Solidity ratio, Sn, Reynolds number, Rn and angle of attack, α, based on experiments by Rudi *et al.* (1988), are presented. In the experiments, nets with square mesh and knots (see Fig. 8) were used with the following properties for $Sn = 0.13$, twine diameter, $d_t = 1.830\,[mm]$ and half mesh size $\lambda = 29.0\,[mm]$, for $Sn = 0.144$, $d_t = 1.380\,[mm]$ and $\lambda = 19.5\,[mm]$, for $Sn = 0.184$, $d_t = 1.081\,[mm]$ and $\lambda = 12.0\,[mm]$, for $Sn = 0.243$, $d_t = 1.830\,[mm]$ and $\lambda = 15.5\,[mm]$ and finally for $Sn = 0.317$, $d_t = 1.830\,[mm]$ and $\lambda = 12.0\,[mm]$. The results are presented as non-dimensionalized drag force coefficients, C_{dnet}, by dividing the drag force with $0.5\rho A\,U_\infty^2$, where A is the enclosed area of the net. The following can be seen from the results:

- There is a clear Reynolds number dependency for the drag coefficient.
- The Reynolds number dependency is increasing with increasing Solidity ratio.
- The Reynolds number dependency is decreasing with decreasing angle of attack.

Fig. 9 and 8 show details of two different types of nets that are commonly used. As seen from the pictures the nets are different with respect to material properties and manufacturing, and even though the net in

Fig. 8: Picture of a traditional mesh with knots. Twine diameter $d = 1.2\,[mm]$ and halfmesh opening $\lambda = 10.0\,[mm]$.

Fig. 9 is called a knotless mesh, the connection area (knot part) have shape and physical dimensions different from an idealized knotless connection between intersecting twines. The individual shape of the twine and the knot part will certainly have an influence on the drag on the net. This is an important key to interprete the results in Fig. 6 and 7. A non circular shape of the twine and the knot part will tend to increase the drag coefficient, while a stranded wire type of shape as in Fig. 8 might slightly decrease the drag coefficient (Hoerner, 1965). The largest difference between the actual net and an idealized net structure made up of equivalent cylinders, will be the knot part. In the following these aspect will be discussed further and sought explained.

The change in drag coefficient of the individual parts which make up the net, partly explains the behavior seen in the experimental results by Rudi *et al.* As seen from Fig. 10, in the relevant Reynolds number range between 10^2 and 10^4, the drag coefficient for a cylinder varies approximately between $1.0 - 1.8$ and for

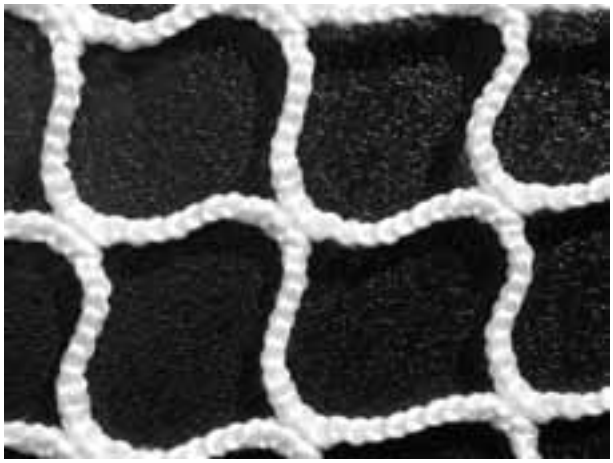

Fig. 9: Picture of a knotless mesh used for aquaculture net pens. Twine diameters $d = 2\,[mm]$ and halfmesh opening $\lambda = 22.5\,[mm]$.

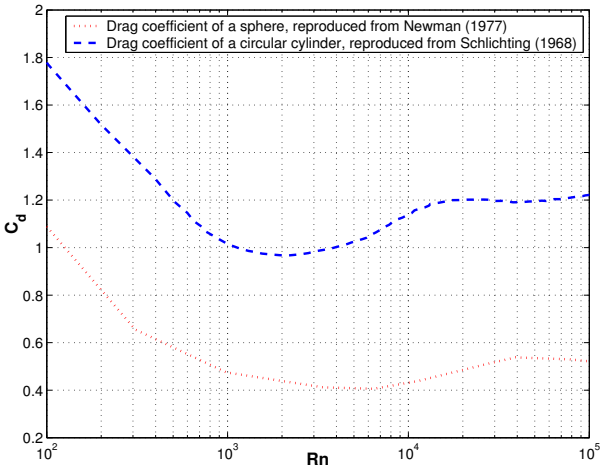

Fig. 10: Drag coefficients of a circular cylinder and a sphere as a function of Reynolds number. Reproduced from Schlichting (1968) and Newman (1977).

a sphere approximately between $0.4 - 1.1$.

In Fig. 11 the experimental results by Rudi *et al.* are plotted together with the ratio, R_{Cdnet}, between the drag force from the experiments and the drag force calculated as a sum of the drag forces on the individual elements, using an equivalent drag force coefficient of a cylinder for the twine and of a sphere for the knot part. The diameter of the knot is taken to be 150% of the diameter of the twine. The following values for the drag coefficient for the twine, C_{dt}, and the knot part, C_{dk}, as a function of Reynolds number were used: $Rn/C_{dt}/C_{dk}$ = 170/1.57/0.85, 212/1.50/0.8, 289/1.35/0.7, 340/1.33/0.62, 436/1.28/0.6, 578/1.15/0.55, 1081/1.0/0.5, 1380/1.0/0.45 and 1830/1.0/0.45. The closer R_{Cdnet} is to 1.0, the more accurate is the assumption that the drag force of the net can be calculated as a sum of the drag forces on

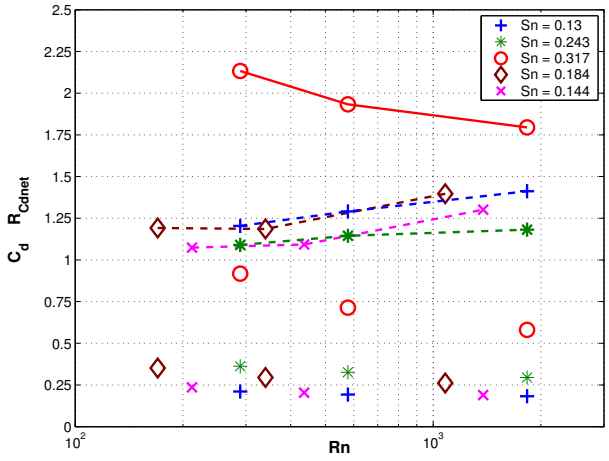

Fig. 11: Drag coefficient for plane nets (markers) and ratios between drag for the net (experiments) and drag calculated as as sum of the drag for individual twine elements (markers and dashed line). Different solidity ratios at 90° angle of attack. Results as a function of Reynolds number.

the individual elements. The results indicate that there is no uniform relation between the drag force on the plane nets used for the experiment and the Solidity ratio. This might be due to differences in the knot part between the different nets, but unfortunately we do not have detailed knowledge of the properties of the net. At the same time it is clear that the results for the highest Solidity ratio, $Sn = 0.317$, deviates the most from a value of $R_{Cdnet} = 1.0$. I.e. when the Solidity ratio increases above a certain value, the drag force on the net can not be treated only as a sum of the drag forces on individual elements. This non-uniform relation between the drag force and the Solidity ratio is noted by several authors, for instance Koritzky (1974) and Fridman (1986), but is not explained. Thus this Solidity ratio dependency of the drag force on a net is not clearly understood.

How the flow is influenced by the knot part is not apparent. It is not enough only to consider the increased area due to the knot part to explain the increasing drag force since the effect is both a function of the Reynolds number and the Solidity ratio. It is likely that there is a flow interaction between the different parts of the net around the knot part. An interaction between "parallel" twines when the angle of attack is larger than approximately 30°, will not occur (Fredheim and Faltinsen, 2002). Even for a relatively high Solidity ratio, say $Sn = 0.5$, the "parallel" twines will be several diameters a part and will be too far apart to influence each other (Zdravkowich, 1985). The relative area of the knot part compared to the total projected area of the net will increase with increasing Solidity ratio and an increasing influence on the drag force is expected. The increased drag force, due to the knot

part of the net, is also supported by results presented in Hoerner (1965). Hoerner indicate an increase in the drag force, called interference drag, due to corners and junction between struts. This interference drag can give an increase in the drag force of up to $20-30\%$ and is dependent both on the shape of the structure and the Reynolds number.

Thus two aspects are to be considered. First the drag force on the knot part as an individual element of the net structure and how to account for this based on its shape and physical dimensions. And secondly how the knot part influences the inflow condition and thereby all other elements of the net structure. To account for the influence on the flow due to the knot part, the knot is modeled as a sphere, and handled in the same matter as a twine element. This is further described in Fredheim and Faltinsen (2001).

Both the physical size of the knot part and its drag coefficient is given as an input to the numerical model presented in this paper. The diameter of the sphere needs to reflect the physical properties of the net, and will likely be in the $O(150-200\%)$ of the diameter of the twine. For the twine, either looked up on as a stranded wire or as a cylinder, it is possible to find suitable experimental results for appropriate drag coefficients. According to Hoerner, with a suitable rounding radius, the drag coefficient for a two-dimensional blunt body drops to the level with a circular cylinder. Thus using a circular cylinder is most likely a good approximation for the twines.

It is not that clear what values of the drag coefficient to use for the knot part. According to Fig. 3.26 in Hoerner (1965) the drag coefficient for a three-dimensional circular and square plate, at Reynolds number between 10^2-10^6, changes from approximately 2.0 to 1.17 with a local maximum of approximately 3.0. Similar the drag coefficient of a three-dimensional cube at Reynolds numbers between 10^4-10^6 is 1.05. Further, the drag coefficient of a blunt body, is largely dependent on any possible rounding radius of its shape.

It is evident that the knot part have a large influence on the drag force and must be accounted for when analyzing a net structure of this type, but it is not clear what drag coefficient to use. We believe it is justified by this discussion and the numerical results presented, that depending on the Solidity ratio and geometry of the knot part, it could be correct to use a drag coefficient in the range of $1.0-2.0$ when modeling the knot part as sphere.

In Fig. 12, 13 and 14 the experimental results by Rudi *et al.* for $Sn = 0.130$, $Sn = 0.243$ and $Sn = 0.317$ are presented together with different numerical results for the drag coefficient of a plane net. These numerical results are obtained by calculating the drag as a sum of the drag of equivalent cylinders and spheres and as a sum of the drag of equivalent cylinders and spheres, including flow correction, based on the method described in Section 2. Dimensions used for the numerical models

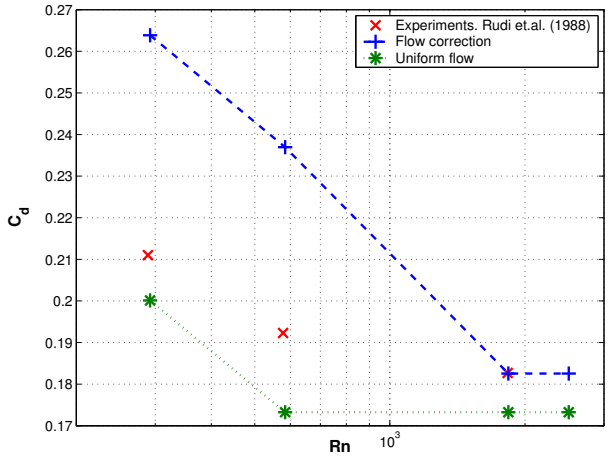

Fig. 12: Drag coefficient for a plane net with $Sn = 0.130$ as a function of Reynolds number at 90° angle of attack. The knot diameter is equal to 150% of the twine diameter, C_d for the twine is Rn dependent and C_d for the knot is 1.5.

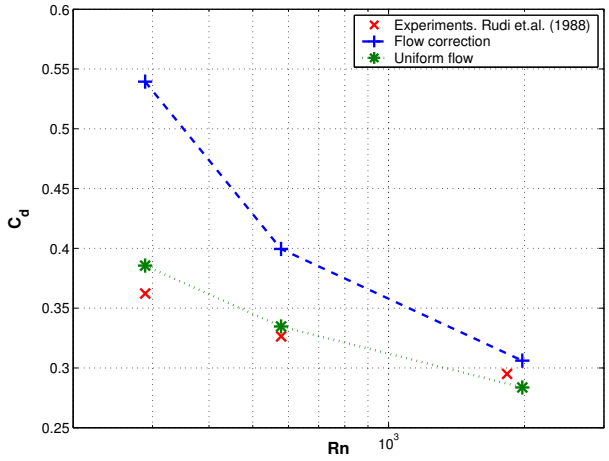

Fig. 13: Drag coefficient for a plane net with $Sn = 0.243$ as a function of Reynolds number at 90° angle of attack. The knot diameter is equal to 150% of the twine diameter, C_d for the twine is Rn dependent and C_d for the knot is 1.0.

were half mesh size $\lambda = 75.0\,[mm]$ and twine diameter $d_t = 4.8\,[mm]$, $d_t = 9.1\,[mm]$ and $d_t = 11.9\,[mm]$ for $Sn = 0.130$, $Sn = 0.243$ and $Sn = 0.317$, respectively.

Due to the non-uniform relation between the drag force on the net and the Solidity ratio the different method gives different agreement with the experiments, depending on the Solidity ratio. For $Sn = 0.243$ the sum of the individual elements, with a drag coefficient for the knot part, $C_{dk} = 1.0$, and without any flow correction, gives good agreement. For $Sn = 0.13$, with, a higher $C_{dk} = 1.5$, the sum of the individual elements gives relatively good agreement. In both cases the flow correction over-predicts the results. Looking at Fig. 11

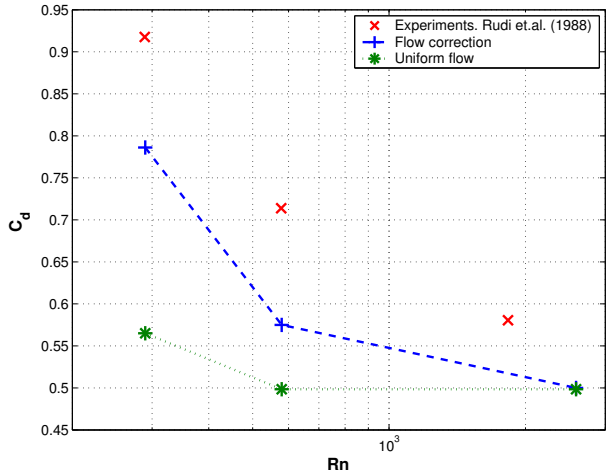

Fig. 14: Drag coefficient for a plane net with $Sn = 0.317$ as a function of Reynolds number at 90° angle of attack. The knot diameter is equal to 150% of the twine diameter, C_d for the twine is Rn dependent and C_d for the knot is 2.0.

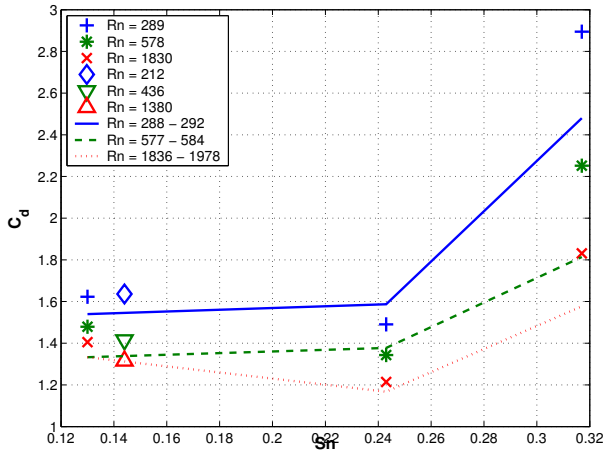

Fig. 15: Drag coefficient for a plane net with at different Reynolds numbers, as a function of Solidity ratio at 90° angle of attack. Markers indicate experimental results (Rudi et.al, 1988) and lines numerical results.

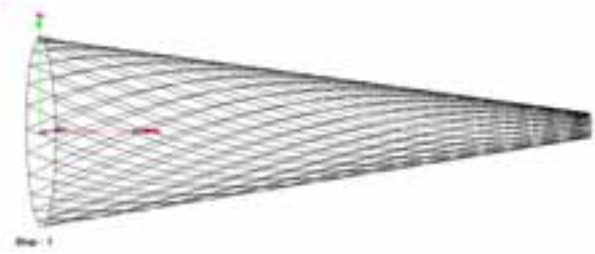

Fig. 16: Illustration of the conical net structure used for numerical analysis.

this is expected since the ratio R_{Cdnet} for both cases are not to far from one and it is closest to 1.0 for $Sn = 0.243$. And finally for $Sn = 0.317$, which have the lowest R_{Cdnet} ratio, it is the results obtained with flow correction that gives the best agreement. This is not expected only by considering R_{Cdnet}, but also due to the fact the results for $Sn = 0.317$ is the most Reynolds number dependent and thus a flow interaction model is expected to give better results.

In Fig. 15 the experimental results by Rudi *et al.* are plotted together with the same numerical results as in Fig. 12, 13 and 14. The results are presented as non-dimensionalized drag force coefficients, C_{dp}, by dividing the drag force with $0.5\rho A_p U_\infty^2$, where A_p is the projected area of the net. For $Sn = 0.13$ and $Sn = 0.243$ it is the "Uniform flow" results which are shown and for $Sn = 0.317$ the "Flow correction" results. Presenting the results by non-dimensionalized with the projected area, A_p, instead the total area, A, removes the inherited Solidity ratio dependency of the drag coefficient, C_{dnet}. It is clear from the figure that at a certain Solidity ratio, there is a strong increase in the drag force. At the same time it seems like the drag coefficient, C_{dp}, tend towards an asymptotic value, when $Sn \to 0$, independent of Solidity ratio. The Reynolds dependency of the drag force is also decreasing, as previously commented. Unfortunately results for lower and higher Solidity ratios are not available. This could contribute to a better understanding of the physics involved.

3.2 *Three-dimensional Net Structures*

Numerical calculations have also been carried out for a cone of 2.94 [m] length, a circular front opening with a diameter of 1.0 [m] and an aft opening of 0.13 [m]. Flow-structure interaction was accounted for by modeling the net structure as a FEM model and finding the mean equilibrium position of the net.

The cone was modeled, using diamond type of meshes, with 20 sections in the longitudinal direction and 25 around the circumference. The twines were modeled as cylinders with a diameter of $1.0\,[cm]$ and drag coefficient $C_{dt} = 1.2$, the knot part as spheres with diameter of $1.5\,[cm]$ and drag coefficient $C_{dk} = 2.0$. With these properties we get a Solidity ratio, $S_n = 0.17$, a mesh opening, $2\phi = 46.3°$ and a mesh size, $l_m = 32.0\,[cm]$ at the front and $S_n = 1.23$ (physically the twines will stock on top of each other), $2\phi = 6.3°$ and $l_m = 29.2\,[cm]$ at the aft. A weighted average Solidity ratio can be calculated with respect to the front and aft circumference of the cone model, and we get $Sn_{av} = 0.29$. The undisturbed current flow was equal to 1.0, and then $Rn = 8.7 \times 10^3$. An illustration of the cone is given in Fig. 16. The results for the total drag force, F_{Dcone}, then becomes $135.4\,[N]$, when no flow correction is applied and $142.7\,[N]$, with flow correction.

Unfortunately there are not much published results regarding analysis of drag forces on three-dimensional

net structures like this. Gustafson (1980), has done towing tank experiments with scale models of trawls, measuring drag forces. The results by Gustafson are non-dimensionalized by $1/2\rho\, A_p U^2$, where A_p is the projected area of the net. The presented numerical method, compared to Gustafson, under-predict the drag force by $10-20\%$. It is not clear what conditions and properties the results by Gustafson are based on. Therefore it is difficult to give a good assessment of the differences in the results. In addition to the uncertainties related to the previously discussed issues regarding the choice of drag coefficients and the influence of the knot part, there is a clear possibility of hydroelastic effects related to fluttering or galloping (Blevins, 1990). A net structure is highly flexible with low structural damping. The possibility of galloping could be due to the non-circular shape of the twines and knots or that one twine could be situated in the wake of another twine. In addition, it is possible that the problem should be investigated as a large scale net structure problem, rather than as a possible small scale, single element phenomena. The presented method assumes a steady state situation, thus even though structural analysis is included, any galloping instabilities will not be predicted. This should be further investigated. It should be pointed out that due to the flexibility of the structure, slow convergence is a problem with the numerical model.

Another possible explanation for the discrepancy is that the results by Gustafson are based on models of trawls, which have a more complex geometry, and that there is a geometrical dependency of the drag force, which is not properly taken care of when the results are non-dimensionalized. Some variation in the drag force coefficient between the different models are also noted. I.e. the results by Gustafson should only be taken as an indication of the level of the drag force and in this view our results seem to reasonable. The results by Gustafson also show a Reynolds number dependency of the drag force, especially at lower Reynolds number, as is the case with the plane net structures. Unfortunately at present we do not have any numerical results for the cone model at lower Reynolds numbers to present.

Kowalski (1974) suggests a relation between the drag force on a conical net structure with a circular opening and the drag force on a plane net panel,

$$F_{Dcone} = \frac{1}{2}\rho C_{dpf} A_f S_n U^2 \qquad (6)$$

where A_f is the area of the circular opening of the cone and C_{dpf} is the drag coefficient for a flat net panel based on the projected area of the net, with the same mesh characteristics as the cone. Using the drag coefficient from the experiments discussed previously, for $Sn = 0.317$ and $Rn = 1830$, and correct it for the projected area instead of the total area enclosing the net, the drag coefficient $C_{dpf} = 1.83$. Then according to the equation, $F_{Dcone} = 208.4$. Further this give us

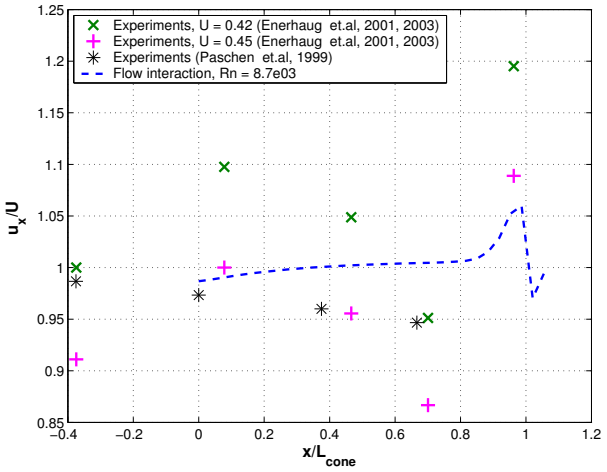

Fig. 17: Velocity profiles along center line of the cone. Experiments by Paschen deviates in terms of geometry.

a drag coefficient, $C_{dp} = 0.28$. This is approximately 20% above the values presented by Gustafson. One reason for the the higher drag force might be that we used the drag coefficient for a net with $Sn = 0.317$, which is above the average Solidly ratio for the cone model.

One of the motivations for this work was to be able to analyze the velocity field within a trawl or a three-dimensional net structure. In Fig. 17 numerical results for the velocity along the center line of the cone, compared to experimental results by Paschen and Winkel (1999), Enerhaug and Gjøsund (2001) and Enerhaug (2003), are presented. The experiments by Enerhaug and Gjøsund are carried out with a cone with the same outer dimensions as the one used for our numerical analysis and with a twine diameter, $d_t = 1.3\,[mm]$ and a mesh size $l_m = 22.0\,[mm]$. In the experiments, the Solidity ratio was kept constant along the cone at $Sn = 0.58$ by reducing number of meshes along the cone.

As seen in the figure, the agreement is not too good. The increased outflow noted by Enerhaug and Gjøsund is also evident in our results, but the reduced flow inside the trawl, seen in both the experimental results, is not recreated in our numerical results. There are a few possible explanation to the discrepancy:

- The difference in the Solidity ratio between the numerical and the experimental model, is significant in the front part. This will lead to less restriction of the flow in the front part. One might then expect a higher increase in the velocity at the outlet of the flow in the numerical model, where the Solidity ratio is higher than in the experimental model. The reason why this is not experienced could also be due to the low Solidity ratio in the front part, because less water is then forced inside the cone.
- The Reynolds number for the experiments by

Enerhaug and Gjøsund was equal to 565, compared to 8.7×10^3 in the numerical analysis. Since there is a large Reynolds number dependency of the drag force on a net structure, it is expected that this is also the situation for the fluid velocity.

- In the experiments by Enerhaug and Gjøsund, the cone longitudinally contracted by approximately 20 $[cm]$ at the aft, giving the cone a more "balloon" type of shape compared to the original shape of the cone. Since this is the case, it is also expected that the mesh opening will decrease. This could lead to a larger restriction of the water flow, and thus the experienced reduction in flow velocity in the middle part of the trawl. The numerical results did not recreate this behavior.
- The numerical model is created using diamond meshes, where each of the twines are continues in a spiral fashion, from the front to the aft part of the cone, as can be seen in Fig. 16. When forces are applied, this modeling might lead to a longitudinal extraction of the cone and thereby a contraction of the circumference, restricting the cone from getting a "balloon" type of shape as noted in the experiments. In a real conical net structure or trawl, this will not occur in the same matter, since to keep the Solidity ratio constant, meshes are "taken off" along the length of the net. I.e. no single twine will be continues in a spiral fashion, as in the numerical model, from the front part to the aft part, but will intersect with other twines, giving the net structure a different geometrical elasticity than the idealized numerical model. And this will lead to a different distribution of the forces. This has to be investigated further.
- There are uncertainties related to which inflow velocity to use for the results by Enerhaug and Gjøsund. Looking at the measurements in front of the cone, in what should be undisturbed water, there is a velocity profile ranging from 0.4 $[m/s]$ at the bottom, up to 0.5 $[m/s]$ close to the surface of the measurement tank. This could give rise to inaccuracy in the experimental results.
- The exact geometry and conditions from the experiments by Paschen and Winkel are not clear. These results should be taken only as an indication.

4 CONCLUSIONS

An examination of numerical results for the drag force on plane net structure demonstrates a strong dependency of the drag force on a net structure with both the geometry, in terms of Solidity ratio and the Reynolds number. This relation is noted by several authors, but is not explained. The dependency is partly due to the change in the drag coefficient for the individual elements which make up a net structure, such as the twine and the knot. Further it is evident that for increasing Solidity ratios, flow interaction will become increasingly significant. The physical design of the knot part contributes largely to this flow interaction, and has an increasing importance as the Solidity ratio increases and the relative area of the knot part compared to the total projected area of the net increases.

A method is presented to calculate the drag force on net structures with high solidity, which gives reasonable good agreement for plane nets and three-dimensional conical net structures. The method uses appropriate drag coefficients related to the geometry of the twines and the knots and account for the change in the inflow due to the presence of the net structure and at the same time changes the geometry of the net structure due to the load.

Also results for a three-dimensional conical net structure are presented. Unfortunately there is not much published results related to analysis of three-dimensional net structures, but compared to results by Gustafson (1980), our numerical results for the total drag force on the cone seem to be reasonable. But the model is not able to predict the correct fluid velocity in front and inside of a three-dimensional net structure, compared to results by Enerhaug and Gjøsund (2001) and Enerhaug (2003). The numerical model seems to be able to recreate some of the characteristics of the flow, but not a noted reduction in the middle part of the structure. The significance of the geometrical elasticity of the net structure for the results, should be further investigated.

To further understand the drag force dependency of the Solidity ratio and Reynolds number and to be able to calculate it in a better manner, it is necessary to understand the physics of the flow around the knot part of the net. Thus further investigation and experimental studies should be carried out, to get a better insight of the flow in the vicinity and around the knot part of the net.

REFERENCES

Blevins, R. D., 1990, *Flow-Induced Vibration*, Van Nostrand Reinhold.

Enerhaug, B., 2003, "Current flow through and aorund conical strctures", Technical Report STF80 A033035, SINTEF Fisheries and Aquaculture. (In Norwegian).

Enerhaug, B. and Gjøsund, S. H., 2001, "Experimental, numerical and analytical studies of flow through reticulate and solid cones", *Proc. of the 5th International Workshop "DEMaT 01"*, University of Rostock, Germany.

Fredheim, A. and Faltinsen, O. M., 2001, "A numerical model for the fluid structure interaction of a three-dimensional net structure", *Proc. of the 5th International Workshop "DEMaT 01"*, University of Rostock, Germany.

Fredheim, A. and Faltinsen, O. M., 2002, "Current forces on net structures", *Proc of The Fifth International Conference on Hydrodynamics*, Tainan, Taiwan.

Fridman, A. L., 1992, *Calculations for fishing gear design*, Fishing News Books Ltd.

Gustafson, T., 1980, "Theoretical and experimental analysis of pelagic trawl", PhD thesis, Dept. of Marine Design, Norwegian Institute of Technology, Norway. (In Norwegian).

Hoerner, S. F., 1965, *Fluid-dynamic Drag*, Hoerner Fluid Dynamics.

Koritzky, H. H., "Beitrag zur Bestimmung von Widerstand und Auftrieb ebener Netztücher", PhD thesis, Unversity of Rostock, Rostock, Germany. (In German).

Kowalski, T. and Gianotti, J., 1974, "Calculation of trawling gear drag", Technical report, Rhode Island University, Kingston, Department of Ocean Engineering.

Newman, J. N., 1977, *Marine Hydrodynamics*, MIT Press.

Paschen, M. and Winkel, H-J., 1999, "Flow investigations of net cones", *Proc. of the 4th International Workshop "DEMaT 99"*, University of Rostock, Germany.

Rudi, *et al.*, 1988, "Experiemnts with nets; forces on and flow trough net panels and cage systems", Technical Report MT 51 F88-0215, MARINTEK, Trondheim, Norway. (In Norwegian).

Schlichting, H., 1968, *Boundary-Layer Theory*, McGraw-Hill.

Winkel, H-J and Paschen, M., 2001, "Wind tunnel test for fishing gear development - methods and limits", *Proc. of the 5th International Workshop "DEMaT 01"*, University of Rostock, Germany.

Zdravkovich, M. M., 1985, "Forces on pipe clusters", *Proc. Conf. Sep. Flow around Marine Structures.*, Norwegian Institute of Technology, Trondheim.